J Mater Sci: Mater Electron (2013) 24:1105–1111
DOI 10.1007/s10854-012-0888-1

Effects of annealing on thermoelectric properties of Sb_2Te_3 thin films prepared by radio frequency magnetron sputtering

Bo Fang · Zhigang Zeng · Xiaoxia Yan · Zhiyu Hu

Received: 10 June 2012 / Accepted: 24 August 2012 / Published online: 5 September 2012
© Springer Science+Business Media, LLC 2012

Abstract Antimony telluride (Sb_2Te_3) thin films were deposited on silicon substrates at room temperature (300 K) by radio frequency magnetron sputtering method. The effects of annealing in N_2 atmosphere on their thermoelectric properties were investigated. The microstructure and composition of these films were characterized using scanning electron microscopy, energy dispersive X-ray spectroscopy and X-ray diffraction, respectively. The electrical transport properties of the thin films, in terms of electrical conductivity and Seebeck coefficient were determined at room temperature. The carrier concentration and mobility were calculated from the Hall coefficient measurement. Both of the Seebeck coefficient and Hall coefficient measurement showed that the prepared Sb_2Te_3 thin films were p-type semiconductor materials. By optimizing the annealing temperature, the power factor achieved a maximum value of 18.02 μW cm^{-1} K^{-2} when the annealing temperature was increased to 523 K for 6 h with a maximum electrical conductivity (1.17×10^3 S/cm) and moderate Seebeck coefficient (123.9 μV/K).

Electronic supplementary material The online version of this article (doi:10.1007/s10854-012-0888-1) contains supplementary material, which is available to authorized users.

B. Fang · Z. Hu
School of Materials Science and Engineering, Shanghai University, Shanghai 200072, People's Republic of China

B. Fang · Z. Zeng (✉) · X. Yan · Z. Hu (✉)
Institute of NanoMicroEnergy, Shanghai University, Shanghai 200444, People's Republic of China
e-mail: zgzeng@shu.edu.cn

Z. Hu
e-mail: zhiyuhu@shu.edu.cn

Z. Zeng · Z. Hu
Department of Physics, Shanghai University, Shanghai 200444, People's Republic of China

X. Yan · Z. Hu
Department of Chemistry, Shanghai University, Shanghai 200444, People's Republic of China

1 Introduction

Thermoelectric devices for energy conversion and temperature control have widely exploited in many industrials field. Compared with the conventional mechanical devices, thermoelectric devices have the advantages such as maintenance free, better transient response [1, 2]. A typical application for the energy conversion is a wristwatch, which incorporates the micro-thermoelectric devices and generates electricity from temperature difference between the surface of the body and the inside of the wristwatch [3]. It is possible to extend the range of application of thermoelectric devices by miniaturizing the devices, such as spot cooling of electric devices and DNA amplification [2, 4].

The primary candidate technology for miniaturizing thermoelectric devices is to apply semiconductor-processing technologies including thin film fabrication. The limited presence of thermoelectric devices on the marketplace is mainly the result of low thermoelectric figures of merit ($ZT = S^2\sigma T/\kappa$) for known thermoelectric materials, where S is the Seebeck coefficient, σ is the electrical conductivity, κ is the thermal conductivity, and T is the absolute temperature. A practical thermoelectric material should have high Seebeck coefficient, high electrical conductivity, and low thermal conductivity [5, 6]. However, the interrelated Seebeck coefficient, electrical conductivity, and thermal conductivity make it difficult to improve one transport property without affecting the others [7]. Thus, the key issue of micro-thermoelectric

devices is how to fabricate thin films with high performance by semiconductor-processing technologies.

Bismuth and antimony telluride-based compounds possess excellent thermoelectric properties near room temperature and are predicted to be the best candidates for thermoelectric devices. Antimony telluride (Sb_2Te_3) is a V-VI compound semiconductor with a small band gap. The Sb_2Te_3 crystal structure has a hexagonal conventional unit cell with a layer structure along in the following order: -(Te^1-Bi-Te^2-Bi-Te^1)- [8]. So far, various techniques have been employed to prepare Sb_2Te_3 thin films including flash evaporation [9], metal organic chemical vapor deposition [10], co-evaporation [11], electrochemical method [12], ion beam sputtering [13], and molecular beam epitaxy [14]. To the best of our knowledge, high performance Sb_2Te_3 thin films were always deposited on a heated substrate [11, 15], while it is incompatible with the condition of lift-off process. All of these facts give us motivation to develop alternative deposited techniques of Sb_2Te_3 thin films. In this work, we employ magnetron sputtering method for the deposition of Sb_2Te_3 thin films. Magnetron sputtering method is an improved film deposition technology, which is convenient and easy to integrate with micro-processing technology, and has been widely employed to large-scale fabrication high quality films.

In this study, the Sb_2Te_3 thin films were deposited at room temperature by RF magnetron sputtering and the post-annealing treatment were employed to enhance their thermoelectric properties. The influence of annealing temperature on the structure, chemical composition and the thermoelectric properties of the Sb_2Te_3 thin films were investigated.

2 Experimental

Antimony telluride thin films were prepared on Si (100) substrates at room temperature ($\sim$300 K) by RF magnetron sputtering (PVD75, USA), using high purity (4 N) Sb_2Te_3 alloy as the sputtering target. The substrates were ultrasonically cleaned prior to deposition in acetone, alcohol and deionized water for 10 min, respectively, and then dried by N_2 gas. The chamber vacuum pressure was $<2 \times 10^{-6}$ Torr before deposition. RF power was 20 W and the working pressure was automatically maintained at 3.0 mTorr. A 10 min pre-sputtering was performed before deposition to remove native oxides and contamination on the surface of the Sb_2Te_3 alloy target. The thickness of the thin films was monitored by a quartz crystal sensor during deposition and measured by step profiler (Ambios XP-200, America) after preparation. The post annealing treatments were performed at 373, 423, 473, 523 and 573 K for 6 h under N_2 atmosphere, respectively. In order to investigate the effect of annealing time, the as-deposited films were also annealed at 523 K for 3, 6, 9 and 12 h, respectively.

The crystal structure of the Sb_2Te_3 thin films was examined by X-ray diffraction (D/MAX-2200, Japan) in conventional θ-2θ mode with Cu/Kα radiation using 40 kV and 250 mA. The specimens were scanned from 20° to 80° with a step of 0.02°. The surface morphology of the thin films was observed by scanning electron microscope (ZEISS ULTRA55, German). Energy dispersive X-ray spectroscopy (EDS) was employed to analyze the chemical compositions of the films.

The carrier concentration and mobility were measured at room temperature by means of Hall coefficient measurement (HMS-3000, Korea). The electrical conductivity of the thin films was measured at room temperature by four-probe method. The in-plane Seebeck coefficient was obtained by a home-made measurement system at room temperature (Fig. 1). A temperature difference (about 5 K) was built up for Seebeck coefficient measurement by putting a heater with a constant current controller under one side of a specimen, and two Pt-100 platinum resistances were used as the thermocouples to monitor the temperature. The distance between the thermocouple was 1 cm. The induced thermal voltage was captured by a data acquisition/switch unit (34970, Agilent, USA). The mechanical pressure was used to ensure the thermal and electrical contacts quality. The Seebeck coefficient was calculated as the ratio of the Seebeck voltage (ΔV) across the thin film to the temperature difference (ΔT, below 5 K) at room temperature. The thermoelectric power factor was estimated from the results of the Seebeck coefficient and electrical conductivity.

3 Results and discussion

3.1 Structural analysis

The surface morphologies of the Sb_2Te_3 thin films were investigated by SEM (Fig. 2). As can be seen in Fig. 2a and b, the grain boundary of annealed film (423 K) was

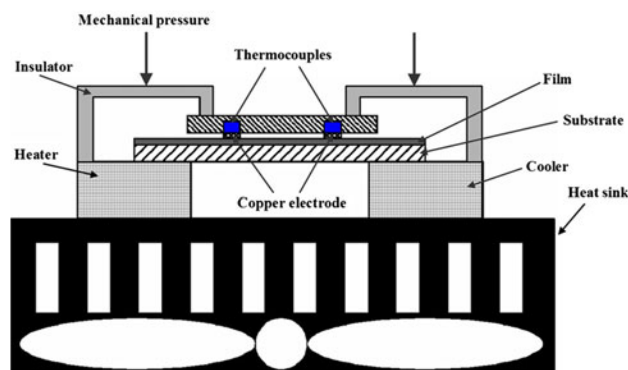

Fig. 1 Schematic of experimental set-up for Seebeck coefficient measurement

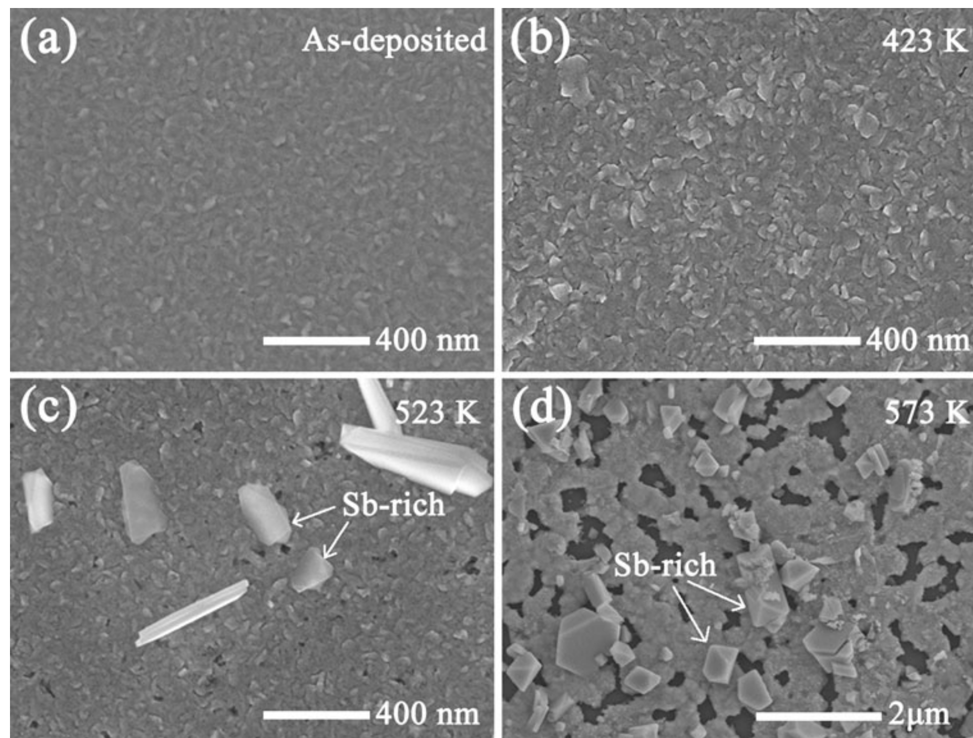

Fig. 2 SEM micrographs of **a** as-deposited Sb_2Te_3 thin film and films annealed at **b** 423 K, **c** 523 K and **d** 573 K for 6 h under N_2 atmosphere, respectively

much clearer than that of as-deposited film, and the surface of the film annealed at 423 K was more uniform. Some crystalloid precipitates and nano-voids (about 20 nm) were found on the surface of the thin film annealed at 523 K, as shown in Fig. 2c. The crystalloid precipitates were examined by EDS analysis and were found to have higher Sb content than the average film composition. The Sb-rich phase has a composition close to Sb:Te = 82:18. A similar Sb-rich precipitates had also been reported in annealed Bi-Sb–Te nanocrystalline thin films [16]. Furthermore, the size and amount of the Sb-rich precipitates were both increased when the annealing temperature increased to 573 K (Fig. 2d). It seems like that Sb atoms are inclined to diffuse to some preferential nucleation site, e.g. grain boundaries, and the nuclei would continue to grow if the Sb atomic flux is sustained. The voids at nano-scale could be formed due to the Sb vacancies or interstices. However, parts of the thin films have been lost at higher annealing temperature due to the separation of substantial Sb-rich precipitates and the consequent disruption of film's structure.

The crystallinity of the Sb_2Te_3 thin films with different annealing temperature was investigated by XRD (Fig. 3). The as-deposited film was almost amorphous structures for the atoms in the film do not have enough energy to diffuse and agglomerate at room temperature. After annealing, three major diffraction peaks were appeared at 2θ of 28.24°, 38.29° and 45.86°, which were assigned to the (015), (1,010), (1,013) planes of Sb_2Te_3, respectively. The result demonstrated that a hexagonal structure belonging to the $R\bar{3}m$ space group of polycrystalline Sb_2Te_3 thin films was obtained [13, 17]. The intensity of Sb_2Te_3 peaks were gradually enhanced when the annealing temperature increased from 373 to 573 K, which suggested that the crystallinity degree of Sb_2Te_3 thin films increased with the rising annealing temperature. However, some new peaks appeared at 32.30°, 52.00°, 67.82° were found when the annealing temperature was 573 K. Compare to the PDF card (26-0101) of Sb, the new peaks at 2θ of 32.30° and 67.82° may belong to Sb (200) and Sb (103) planes, respectively. The peak at 2θ of 52.00° may belong to Te (103) plane (PDF card [36-1452] of Te). The result indicated that there may exist a phase separation at higher temperature of 573 K, where the diffusion, nucleation and growth of Sb atoms in the Sb_2Te_3 thin film. And this was also in accordance with the result in the SEM an image (Fig. 2d). Although there was no noticeable difference of grain size in surface morphology from 423 to 523 K, XRD patterns showed that the grain sizes of the thin films increased with the increase of annealing temperatures. The average grain sizes of the thin films were calculated using the Debye–Scherrer's equation:

$$D = k\lambda/B\cos\theta \quad (1)$$

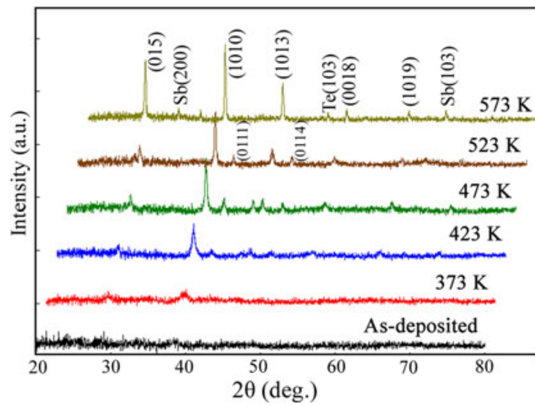

Fig. 3 XRD patterns of the Sb_2Te_3 thin films annealed at different temperatures for 6 h under N_2 atmosphere

Table 1 The average grain sizes of the thin films calculated from (1,010) plane at 2θ of 38.29°

Annealing temperature (K)	FWHM B (°)	$B\cos\theta$	Average grain size D (nm)
As-deposited	–	–	–
373	1.307	0.02142	6.4
423	0.448	0.00710	19.3
473	0.310	0.00479	28.6
523	0.271	0.00410	33.4
573	0.199	0.00280	49.0

where k is the constant = 0.89, λ is the wavelength of the radiation = 1.54051 Å, B is the full-width half-maximum (FWHM) and θ is the diffraction angle. XRD parameters for the specimens were listed in Table 1, which showed the calculated results. It could be found clearly that the average grain sizes were increased with increasing annealing temperature.

Te atomic compositions and the film thickness of the Sb_2Te_3 thin films as a function of the annealing temperature were shown in Fig. 4. It can be found that the Te concentration of the as-deposited thin film was 66 % and the thickness was about 250 nm. Both the Te composition and the film thickness were decreased linearly when the annealing temperature increased to 523 K. This may be due to the re-evaporation of elements Te during annealing treatment [6]. Besides, owing to the evaporation of elements Te, there are less Te_{Sb} native antisite defects (the rich Te atoms occupying Sb lattice sites) in the grain region, and the composition of the thin films is close to the chemical composition ratio. However, when the annealing temperature reached 573 K, the content of Te increased drastically to about 93 %. According to the SEM (Fig. 2d) and XRD patterns (Fig. 3), the thin films were inclined to phase separation at higher annealing temperature of 573 K. Therefore, in our case, some region that without Sb-rich precipitates exhibited higher content of Te; in contrast, other regions showed lower content of Te. See supplementary information for more details on the EDS testing. So the drastically increase of Te content (about 93 %) in Fig. 4a) could be attributed to that we detected the area without Sb-rich precipitates.

3.2 Thermoelectric properties of Sb_2Te_3 thin films

The carrier concentration and mobility were measured by Hall coefficient measurement at room temperature (Fig. 5). Due to the structural deterioration of the thin film annealed at 573 K, the carrier concentration and mobility of the thin films annealed at 573 K were not investigated. Obviously, with the increase of annealing temperature, the carrier concentration decreased while the carrier mobility increased. The carrier concentration decreased from 1.30×10^{20} to 7.71×10^{19} cm^{-3} and the carrier mobility increased from 9.52 to 95 cm/Vs as the temperature increased from 300 to 523 K. In general, the thin films deposited at room temperature contain many defects and require a post thermal treatment to eliminate them. The decrease of the carrier concentration can be attributed to the reduction of the Te_{Sb} native antisite defects during annealing treatment, as seen from Fig. 4a. The increase of carrier mobility can be attributed to the reduction of native antisite defects and grain growth due to the crystallization during the annealing treatment. The increasing grain size (as show in Table 1) can contribute to the decrease of the density of grain boundary, reducing carrier scattering at the grain boundaries. So the carrier mobility increased with annealing temperatures rising.

The electrical conductivity and Seebeck coefficient of the Sb_2Te_3 thin films as a function of the annealing temperatures were shown in Fig. 6. We found that the electrical conductivity of Sb_2Te_3 thin films was enhanced after annealing treatment up to a certain temperature. At further higher annealing temperature the electrical conductivity was drastically decreased due to the structural destruction of Sb_2Te_3 thin films. When the annealing temperature increased from 300 to 523 K, The electrical conductivity increased from 1.98×10^2 to 1.17×10^3 S/cm. The weaker electrical conductivities of as-deposited thin film could be attributed to the poor crystallization, as confirmed by XRD analysis in Fig. 3. The increase of electrical conductivity may due to the compensation of the decrease in carrier concentration with the increase in mobility. The electrical conductivity is given by equation:

$$\sigma = ne\mu \tag{2}$$

where n is the carrier concentration, e is the electron charge, μ is the carrier mobility. As seen from Fig. 5, the increase rate of the carrier mobility was higher than the

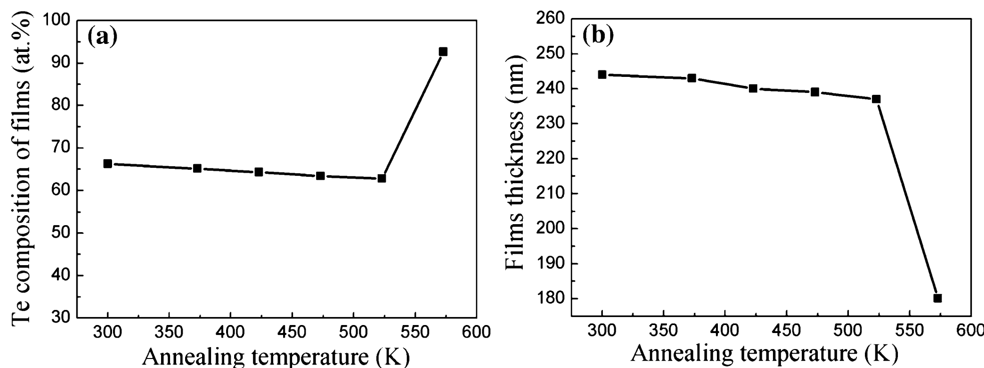

Fig. 4 Te composition and film thickness as a function of annealing temperature

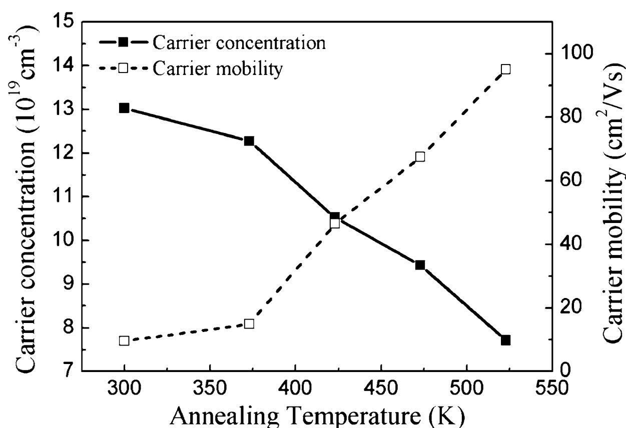

Fig. 5 A plot of the carrier concentration and mobility of the Sb_2Te_3 thin films as a function of annealing temperature

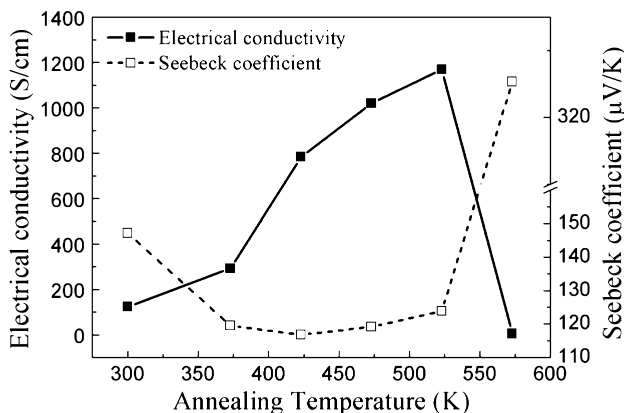

Fig. 6 A plot of the electrical conductivity and the Seebeck coefficient of the Sb_2Te_3 thin films as a function of annealing temperature

decrease rate of carrier concentration. Therefore, the electrical conductivity of the Sb_2Te_3 films was enhanced with the rising annealing temperature.

To measure the in-plane Seebeck coefficient, a small temperature difference (about 5 K) was built up across the specimen to produce Seebeck voltage at room temperature by a home-made Seebeck coefficient measurement system. As shown in Fig. 6, it can be found that the Seebeck coefficients of all the specimens have positive value, indicating that the deposited Sb_2Te_3 thin films are p-type. When the annealing temperature was increased to 423 K, the Seebeck coefficient decreased a lot compared with that of the film annealed at 300 K. The sharp fall in the Seebeck coefficient can be explained with amorphous-crystalline transition. The similar result for Sb_2Te_3 thin films prepared by evaporation was also reported by V. Damodara et al. [18]. Nevertheless, the Seebeck coefficient increased slightly while annealing temperature was further raised from 423 K. It is well known that the Seebeck coefficient is closely related to the carrier concentration. In the case of p-type semiconductor crystals obeying Boltzmann statistics, the Seebeck coefficient is given by equation:

$$S = (k/e)[r + C - \ln n] \tag{3}$$

where k is the Boltzmann's constant, e is the electron charge, r is the scattering parameter and the value of r is dependent on the scattering mechanism ($r = -1/2$ for lattice scattering and $r = 3/2$ for ionized scattering), and C is a constant [19, 20]. The Seebeck coefficient was found to be inversely proportional to the logarithmic scale of the carrier concentration. The reason for the enhancement of Seebeck coefficient is the reduction of carrier concentration. However, the Seebeck coefficient of the thin films annealed at 573 K increased drastically (about 330 μV/K), which was close to that of Te films [21]. As can be seen from Fig. 2d, the substantial Sb-rich precipitates on the surface are almost discontinuous, so the main contribution to the Seebeck coefficient maybe the rich Te phases in the films. Thus, the thin films annealed at 573 K have relative higher Seebeck coefficient but lower electrical conductivity.

The power factor ($S^2\sigma$) of Sb_2Te_3 thin films has been calculated by the measured Seebeck coefficient and electrical conductivity (Fig. 7). The as-deposited thin films have the value of about 4.29 μW cm^{-1} K^{-2}. After the annealing treatment, the power factors were increased by an order of magnitude. The largest value of the power

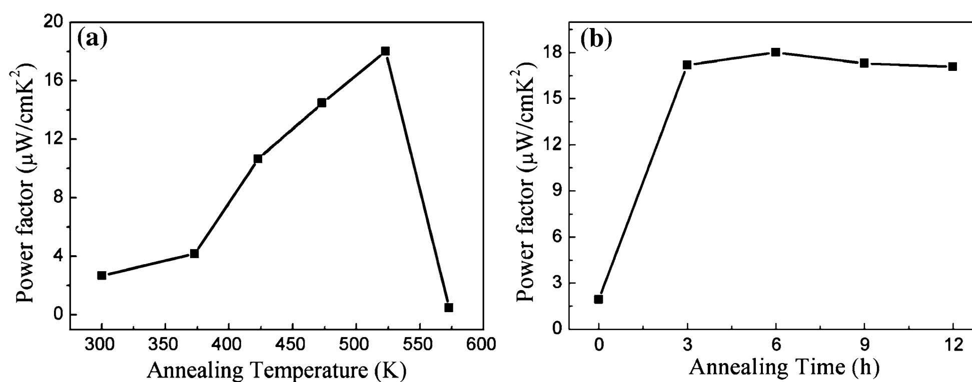

Fig. 7 A plot of the power factor of the Sb_2Te_3 films as a function of annealing temperature

factor ($\sim$18.02 μW cm^{-1} K^{-2}) was obtained for the stoichiometric specimen annealed at 523 K. Even though the higher temperature such as 573 K may lead to the deterioration of thermoelectric properties of the films, the annealing treatment was testified to be a kind of very efficient method to improve the properties of the thermoelectric thin films.

In order to further optimize the annealing parameters on the Sb_2Te_3 thin films, an annealing treatment was performed in N_2 atmosphere for different times at 523 K. Thermoelectric power factors as a function of the annealing time are shown in Fig. 7b. It can be found that the power factor has slightly changed in a range of 17.19–18.02 μW cm^{-1} K^{-2}. The annealing time has no significant effects on the thermoelectric properties of Sb_2Te_3 films. Therefore, we suggest that annealing temperature is a key factor on thermoelectric properties according to our experimental results.

4 Conclusions

The Sb_2Te_3 thin films were successfully deposited by RF magnetron sputtering on silicon substrates. In order to enhance the thermoelectric properties of the thin films, annealing in N_2 atmosphere was carried out for 6 h in the temperature range from 373 to 573 K. The as-deposited films were nearly amorphous and the crystalline quality increase gradually after annealing treatments. Meanwhile, the Sb atoms are inclined to diffuse to form Sb-rich precipitates. But too high annealing temperature may lead to the separation of substantial Sb-rich precipitates and consequent disruption of film's structure. It is found that with the increase of annealing temperature, the carrier concentration decrease while the carrier mobility increases. In summary, the annealing treatment may effectively improve the thermoelectric properties of the Sb_2Te_3 thin films. The power factor of the films reach the highest value of 18.02 μW cm^{-1} K^{-2}, which is annealed at 523 K for 6 h with a maximum electrical conductivity (1.17×10^3 S/cm) and moderate Seebeck coefficient (123.9 μV/K). This is very promising in the realization of room temperature thermoelectric application with high performances.

Acknowledgments This research was supported by Shanghai Science and Technology Funds (10520710400, 10PJ1403800, 11DZ1111200), Yunnan Provincial Science and Technology Department (2010AD003), National Natural Science Foundation of China (21103104, 61204129), Innovation Foundation of Shanghai University and the Special Fund for Selection and Cultivation Excellent Youth in the University of Shanghai city.

References

1. Y. Zhang, J. Christofferson, A. Shakouri, G.H. Zeng, E. John Bowers, IEEE Trans Compon Packaging Technol **29**, 395–401 (2006)
2. I. Chowdhury, R. Prasher, K. Lofgreen, G. Chrysler, S. Narasimhan, R. Mahajan, D. Koester, R. Alley, R. Venkatasubramanian, Nat Nanotechol **4**, 235–238 (2009)
3. M. Kishi, H. Nemoto, T. Hamao, M. Yamamoto, S. Sudou, M. Mandai, S. Yamamoto, Proceedings of 18th International Conference on Thermoelectrica, 301–304 (1999)
4. K. Shen, X. Chen, M. Guo, J. Cheng, Sens Actuators B **105**, 251–258 (2005)
5. Y. Du, K.F. Cai, S.Z. Shen, B. Qin, P.S. Casey, J Mater Sci Mater El **23**, 870–876 (2011)
6. X.K. Duan, Y.Z. Jiang, Appl Surf Sci **256**, 7365–7370 (2010)
7. K.M. Liou, C.N. Liao, J Appl Phys **108**, 1–5 (2010)
8. M.H. Francombe, Br J Appl Phys **9**, 415–418 (1958)
9. N.G. Patel, P.G. Patel, J Mater Sci **26**, 2543–2546 (1991)
10. R. Venkatasubramanian, T. Colpitts, E. Watko, M. Lamvik, N. El-Masry, J Cryst Growth **170**, 817–821 (1997)
11. H.L. Zou, D.M. Rowe, S.G.K. Williams, Thin Solid Films **408**, 270–274 (2002)
12. İ.Y. Erdoğan, Ü. Demir, J Electroanal Chem **633**, 253–259 (2009)
13. P. Fan, Z.H. Zheng, G.X. Liang, X.M. Cai, D.P. Zhang, Chin Phys Lett **27**, 087021 (2010)
14. Y.K. Kim, A. Divenere, G.K. Wong, J.B. Ketterson, S. Cho, J Appl Phys **91**, 715–718 (2002)
15. L.M. Goncalves, P. Alpuim, A.G. Rolo, J.H. Correia, Thin Solid Films **519**, 4152–4157 (2011)
16. C.N. Liao, K.M. Liou, H.S. Chu, Appl Phys Lett **93**, 1–3 (2008)
17. T.B. Chen, P. Fan, Z.H. Zheng, D.P. Zhang, X.M. Cai, G.X. Liang, J.R. Chi, Adv Mat Res **194–196**, 2400–2403 (2011)

18. V. Damodara Das, N. Soundararajan, M. Pattabl, J Mater Sci **22**, 3522–3528 (1987)
19. A.F Ioffe, Semiconductor Thermoelements and Thermoelectric Cooling, 1st ed, Infosearch, 18–40 (1957)
20. M. Takashiri, T. Shirakawa, K. Miyazaki, H. Tsukamoto, J Alloys Compd **441**, 246–250 (2007)
21. V. Damodara Das, N. Jayaprakash, N. Soundararajan, J Mater Sci **16**, 3331–3334 (1981)